Appl. Phys. B 68, 225–232 (1999)

Applied Physics B
Lasers
and Optics

Resonant absorption and scattering in evanescent fields

R. Wannemacher*, **A. Pack, M. Quinten**

Institute of Physics, Chemnitz University of Technology, Reichenhainer Str. 70, D-09107 Chemnitz, Germany

Received: 14 July 1998

Abstract. The enhancement of optical resonances of small spherical particles in the case of excitation by evanescent waves is investigated. This enhancement is due to the large intensity gradient of the excitation and depends strongly on the decay length of the evanescent wave as well as on its polarisation. Resonances due to excitations of the bulk material are considered as well as morphology-dependent resonances due to constructive interference of circumpropagating waves in dielectric particles. In the important case, when the particle is in contact with a surface, where the evanescent wave is generated by total internal reflection, both types of resonances are attenuated, broadened, and redshifted due to multiple scattering processes. These effects have been studied by means of the numerical multiple multipole (MMP) method. It is found that even in this case strong enhancement of resonances due to higher multipoles is retained, corresponding to scattering and absorption spectra significantly different from those for plane-wave excitation. Multiple scattering processes are found to become inefficient when the distance of the particle to the surface exceeds about the particle radius.

PACS: 42.25.Fx; 78.40.-q

Scattering and extinction of light by small particles have been studied for almost a century, and the classical theory initially developed by Gustav Mie [1] has found widespread applications in many fields of science and engineering. In this standard theory, the incident and scattered fields, as well as the fields inside a spherical particle are developed into series of transverse electric and magnetic multipoles. Depending on the size and complex refractive index of the particle, resonances are observed as a function of wavelength, which arise from the poles of the various multipolar contributions in the series. It was noted recently, that these resonances, especially those of higher order, may be strongly enhanced in the case of evanescent-wave excitation as compared to plane-wave excitation [2]. Such size-dependent resonances show prospect of practical applications, for example for size determination or sorting of small particles. Furthermore, all experiments, where strong local fields enhance optical properties of a sample, may benefit from resonance enhancements in evanescent fields. This applies to, for example, surface-enhanced Raman scattering, or nonlinear optical effects, such as second-harmonic generation. It should be emphasized, that similar enhancements of higher-order resonances are generally expected in situations, where the excitation exhibits strong intensity gradients. The current paper is intended to discuss in more detail resonance enhancements in evanescent fields, mainly in the visible spectral range, and the additional effects of multiple scattering at the prism surface.

Obviously, the number of resonances in the visible range and their magnitudes and halfwidths depend on the optical properties of the particle material as well as on size and composition of the particles. For very small particles, i.e. in the Rayleigh limit, only the dipolar contribution is relevant. In this case resonances occur when the complex dielectric function of the particle material approaches certain negative real values, which are in general related to bulk excitations. Quantum size effects, which may lead to resonances in the Rayleigh limit that are different from those of the bulk, are not considered in the current paper. For larger particles so-called morphology-dependent resonances (MDRs) occur, which are not related to bulk excitations and do not require negative values of the dielectric function, but are determined by the size and shape of the particle. Enhancements due to evanescent-wave excitation generally increase with order n, which means that more pronounced effects are observed for larger particles. Even for comparatively small particles with positive values of their dielectric function, however, higher multipoles are important, if the particles are covered with a thin layer of a material, which exhibits a negative dielectric function. In the following, enhancements of resonances of homogeneous spheres and of coated spherical particles will be discussed.

Evanescent optical fields are commonly generated by total internal reflection from the interface between two media of different refractive index. In this case the particle resides in

* Corresponding author. Fax +49-371/531-2692,
E-mail: wannemacher@physik.tu-chemnitz.de

the thinner medium, and, in most experimental setups is in contact with the interface. This complicates the situation considerably because of multiple scattering. The latter leads to pronounced effects, which we discuss below for homogeneous as well as for coated particles.

1 Scattering in evanescent fields

In this section scattering of light by small spherical particles is briefly recalled. The formalism of the theory of light scattering by spheres can be found in readily available monographs and textbooks [3–6]. In 1908 Mie [1] and independently in 1909 Debye [7] solved this problem for an isolated sphere and a plane incident wave. In 1977 Chew et al. [8] treated the problem of scattering of evanescent waves by small particles by analytic continuation of the case of plane-wave excitation. They were primarily interested in the dependence of the differential scattering cross sections on the scattering angle. Their results were recently applied by Liu et al. [9] to MDRs in the differential scattering cross section of dielectric particles. Those authors calculated the size dependence of an unnormalized differential cross section for a specific scattering angle, but mainly studied the intensity distribution inside the sphere. Enhancement of higher multipoles in evanescent-wave scattering seems to have been noticed in a previous study of Barchiesi and van Labeke [10]. These authors considered the diffraction of evanescent waves on a grating from a small sphere and calculated in this way the images of the grating, which would be obtained by scanning tunneling optical microscopy under monochromatic illumination. They were not, however, interested in the effect of the multipolar enhancements on the scattering and extinction spectra, and, in fact, their calculations refer to a case where no resonant features exist in the visible range of wavelengths. Furthermore, neither of the authors mentioned considered the effects of the prism surface on resonances of small particles in the evanescent field. In [2] total cross sections were defined and calculated as a function of the wavelength for the case of small silver particles. The enhancement of contributions from higher multipoles to scattering and extinction, as compared to plane-wave excitation, was shown to lead to significant changes in the scattering and extinction spectra. The influence of the prism surface was investigated for these particles by means of the multiple multipole (MMP) method.

Here we take into account the more general case of coated spherical particles. In 1951 Aden and Kerker [11] and independently in 1952 Güttler [12] extended Mie's theory to particles with one layer. Extension to arbitrary numbers of layers was reported in 1985 by Bhandari [13] using a matrix formalism. A recursive formulation was developed in 1994 by Sinzig and Quinten [14] and is more practicable for generation of computer codes. Also in 1994, but independent of [14], Kai and Massoli [15] developed a similar recursion formalism.

In the following, we briefly repeat the expressions for the optical cross sections obtained in [2]. According to the definition employed in this reference, the cross sections for extinction and scattering of an evanescent wave by a spherical particle with diameter $2a$ are

for s-polarised light:

$$\sigma^{s}_{\mathrm{ext}} = \frac{2\pi}{k_{\mathrm{M}}^2} N^{-1} \,\mathrm{Re} \sum_{n=1}^{\infty} (2n+1)\,(a_n \Pi_n + b_n T_n) \;, \tag{1a}$$

$$\sigma^{s}_{\mathrm{sca}} = \frac{2\pi}{k_{\mathrm{M}}^2} N^{-1} \sum_{n=1}^{\infty} (2n+1)\left(|a_n|^2\,\Pi_n + |b_n|^2\,T_n\right) \;, \tag{1b}$$

for p-polarised light:

$$\sigma^{p}_{\mathrm{ext}} = \frac{2\pi}{k_{\mathrm{M}}^2} N^{-1} \,\mathrm{Re} \sum_{n=1}^{\infty} (2n+1)\,(a_n T_n + b_n \Pi_n) \;, \tag{1c}$$

$$\sigma^{p}_{\mathrm{sca}} = \frac{2\pi}{k_{\mathrm{M}}^2} N^{-1} \sum_{n=1}^{\infty} (2n+1)\left(|a_n|^2\,T_n + |b_n|^2\,\Pi_n\right) \;, \tag{1d}$$

with the definitions

$$\Pi_n(\theta_k) = \frac{2}{n(n+1)} \sum_{m=-n}^{n} \frac{(n-m)!}{(n+m)!} \left| m \frac{P_{nm}(\cos\theta_k)}{\sin\theta_k} \right|^2 \;, \tag{2a}$$

$$T_n(\theta_k) = \frac{2}{n(n+1)} \sum_{m=-n}^{n} \frac{(n-m)!}{(n+m)!} \left| \frac{\mathrm{d}P_{nm}(\cos\theta_k)}{\mathrm{d}\theta_k} \right|^2 \;, \tag{2b}$$

and the coefficients a_n and b_n being the scattering coefficients of the TM modes and TE modes of the spherical particle, respectively. Formulae (1a)–(1d) are valid not only for homogeneous, but also for coated spherical particles with an arbitrary number of layers. Only the expressions for the coefficients a_n, b_n differ in these cases. For an incident plane wave $T_n = \Pi_n = 1$ for all multipolar orders n and angles θ_k with $\cos\theta_k \leq 1$. In this case the cross sections are, of course, equal for s- and p-polarisation and (1) are the well-known results from standard Mie theory. For an incident evanescent wave the functions T_n, Π_n increase with the order n and with the angle of incidence, and can attain very large values [2]. This simply reflects the fact that due to the large intensity gradient the evanescent wave contains much stronger contributions from higher multipoles than an incident plane wave.

The normalisation factor N is equal to one for plane waves, but assumes a different value for evanescent waves. If the cross section is normalized to the total incident power, N is given by [2]

$$N = \frac{n_{\mathrm{P}}}{n_{\mathrm{M}}} \sin\theta_i \frac{\mathrm{I}_1(2\kappa a)}{\kappa a} = \frac{n_{\mathrm{P}}}{n_{\mathrm{M}}} \sin\theta_i \left(1 + \sum_{m=1}^{\infty} \frac{(\kappa a)^{2m}}{m!(m+1)!}\right) . \tag{3}$$

In view of the further discussion of results for coated spheres, it is convenient to quote the coefficients a_n and b_n for a spherical particle coated with a single layer of another material. They are

$$a_n = \frac{\left\{ \begin{array}{r} \Psi_n(x_1)\left[\Psi_n'(m_1x_1) + A_n\chi_n'(m_1x_1)\right] \\ -\, m_1\Psi_n'(x_1)\left[\Psi_n(m_1x_1) + A_n\chi_n(m_1x_1)\right] \end{array} \right\}}{\left\{ \begin{array}{r} \xi_n(x_1)\left[\Psi_n'(m_1x_1) + A_n\chi_n'(m_1x_1)\right] \\ -\, m_1\xi_n'(x_1)\left[\Psi_n(m_1x_1) + A_n\chi_n(m_1x_1)\right] \end{array} \right\}} \;, \tag{4}$$

$$b_n = \frac{\left\{ \begin{array}{l} m_1 \Psi_n(x_1) \left[\Psi_n'(m_1 x_1) + B_n \chi_n'(m_1 x_1) \right] \\ - \Psi_n'(x_1) \left[\Psi_n(m_1 x_1) + B_n \chi_n(m_1 x_1) \right] \end{array} \right\}}{\left\{ \begin{array}{l} m_1 \xi_n(x_1) \left[\Psi_n'(m_1 x_1) + B_n \chi_n'(m_1 x_1) \right] \\ - \xi_n'(x_1) \left[\Psi_n(m_1 x_1) + B_n \chi_n(m_1 x_1) \right] \end{array} \right\}} , \tag{5}$$

with

$$A_n = -\frac{\Psi_n(x_0)\Psi_n'(m_0 x_0) - m_0 \Psi_n'(x_0)\Psi_n(m_0 x_0)}{\chi_n(x_0)\Psi_n'(m_0 x_0) - m_0 \chi_n'(x_0)\Psi_n(m_0 x_0)} , \tag{6}$$

$$B_n = -\frac{m_0 \Psi_n(x_0)\Psi_n'(m_0 x_0) - \Psi_n'(x_0)\Psi_n(m_0 x_0)}{m_0 \chi_n(x_0)\Psi_n'(m_0 x_0) - \chi_n'(x_0)\Psi_n(m_0 x_0)} , \tag{7}$$

and the size parameters

$$x_0 = \frac{2\pi}{\lambda} a_{\mathrm{core}} n_{\mathrm{shell}}(\lambda) \qquad x_1 = \frac{2\pi}{\lambda} \left(a_{\mathrm{core}} + d_{\mathrm{shell}} \right) n_{\mathrm{M}}(\lambda) , \tag{8}$$

and the relative indices of refraction

$$m_0(\lambda) = \frac{n_{\mathrm{core}}(\lambda)}{n_{\mathrm{shell}}(\lambda)} \qquad m_1(\lambda) = \frac{n_{\mathrm{shell}}(\lambda)}{n_{\mathrm{M}}(\lambda)} . \tag{9}$$

Here, λ is the vacuum wavelength of the incident light. $\Psi_n(z) = z j_n(z)$, $\chi_n(z) = z y_n(z)$, and $\xi_n(z) = z h_n^{(1)}(z)$ are Riccati–Bessel, Riccati–Neumann, and Riccati–Hankel functions. The prime denotes the derivative with respect to the argument. These results include the results for a homogeneous sphere, which are obtained either for $a_{\mathrm{core}} = 0$ or $d_{\mathrm{shell}} = 0$.

Resonances occur if the denominators of the scattering coefficients a_n and b_n become small. In this case the corresponding mode will dominate the scattered field. These resonances are caused either by the constructive interference of light waves, that travel just inside a narrow domain in the vicinity of the surface of the sphere (these are the MDRs mentioned above), or by surface excitations which require negative values of the dielectric function of the bulk material. The latter may be due for example to the presence of conduction electrons, excitons, or, in the infrared, to lattice vibrations. For small homogeneous particles or for thin shells the surface excitations just mentioned are the only possible source of resonances. To get morphology-dependent resonances either the particle must be sufficiently large, or, for particles of a given size, the index of refraction must be sufficiently high.

The TM-modes a_n are resonant if

$$m_1 \frac{\xi_n'(x_1)}{\xi_n(x_1)} = \frac{\Psi_n'(m_1 x_1) + A_n \chi_n'(m_1 x_1)}{\Psi_n(m_1 x_1) + A_n \chi_n(m_1 x_1)} , \tag{10}$$

and the TE-mode b_n is resonant if

$$\frac{1}{m_1} \frac{\xi_n'(x_1)}{\xi_n(x_1)} = \frac{\Psi_n'(m_1 x_1) + B_n \chi_n'(m_1 x_1)}{\Psi_n(m_1 x_1) + B_n \chi_n(m_1 x_1)} . \tag{11}$$

Of course, (10) and (11) can be satisfied only approximately for real λ. The resonances of a homogeneous sphere are obtained for $A_n = B_n = 0$. The resonances described by (10) and (11) are the same for plane-wave and evanescent-wave excitations, as (1)–(5) apply to both cases, the difference being different values of the quantities in (2) and (3). Whereas the positions and widths of the resonances are the same in both cases, the amplitudes of resonances corresponding to $n > 1$ are strongly enhanced for evanescent-wave excitation.

In order to study the behavior of very small particles, we simplify these expressions by using the Rayleigh approximation, i.e., for size parameters $x \ll 1$. Then, it can be shown that only the TM-modes are resonant and the resonance condition explicitly reads for each multipolar order n:

$$\left(\varepsilon_{\mathrm{shell}} + \frac{n+1}{n} \varepsilon_{\mathrm{M}} \right) \left(\varepsilon_{\mathrm{core}} + \frac{n+1}{n} \varepsilon_{\mathrm{shell}} \right) + \frac{n+1}{n} \left(\frac{a_{\mathrm{core}}}{a_{\mathrm{core}} + d_{\mathrm{shell}}} \right)^3 \left(\varepsilon_{\mathrm{shell}} - \varepsilon_{\mathrm{M}} \right) \left(\varepsilon_{\mathrm{core}} - \varepsilon_{\mathrm{shell}} \right) = 0 . \tag{12}$$

Here, Maxwell's relation between the index of refraction $\tilde{n}(\lambda)$ and the corresponding dielectric function $\varepsilon(\lambda)$ is used for the core, shell, and surrounding medium. The limiting cases $a_{\mathrm{core}} = 0$ and $d_{\mathrm{shell}} = 0$ result in the condition for a compact sphere ($\varepsilon_{\mathrm{core}} = \varepsilon_{\mathrm{shell}} = \varepsilon$):

$$\left(\varepsilon + \frac{n+1}{n} \varepsilon_{\mathrm{M}} \right) = 0 . \tag{13}$$

2 Spectra of scattering and extinction in evanescent fields

Specific examples for the case of homogeneous spheres and for coated spheres are discussed in the current section. In addition, the range of refractive indices, particle sizes, and thickness of the coating layer is investigated, for which well-defined resonances of multipolar orders $n > 1$ are obtained in the visible spectral range.

2.1 Homogeneous spheres

Obviously, MDRs occur, if the size parameter $ka = n_{\mathrm{M}} 2\pi a/\lambda$ exceeds a value of order unity. This value depends on the real part n' of the complex index of refraction of the particle material and decreases with increasing n'. On the other hand, for particles with diameters above approximately $2a = 5\,\mu\mathrm{m}$ the number of resonances in the visible range becomes very large, which is unfavorable for a number of possible applications. In addition, to obtain well-defined resonances, the imaginary part n'' of the refractive index must not be too large. In the case of semiconductor materials n'' generally decreases in the visible range with increasing wavelength, which means that MDRs are more likely to be observed at longer wavelengths. For some materials, for example germanium or amorphous silicon, large n'' values preclude the existence of MDRs over most of the visible and near infrared range. For crystalline silicon the large value of n' (between 5 and 3.6 at wavelengths between $0.3\,\mu\mathrm{m}$ and $1\,\mu\mathrm{m}$ [16]) gives rise to morphology-dependent resonances for particles with $2a > 0.15\,\mu\mathrm{m}$. In this case, however, n'' is considerably smaller, and sharp resonances appear in the spectra.

As an example, Fig. 1 depicts the optical extinction cross sections of a compact crystalline silicon sphere with $2a = 200\,\mathrm{nm}$ for excitation by a plane wave (Fig. 1a) and for excitation by *p*- and *s*-polarised evanescent waves (Fig. 1b,c).

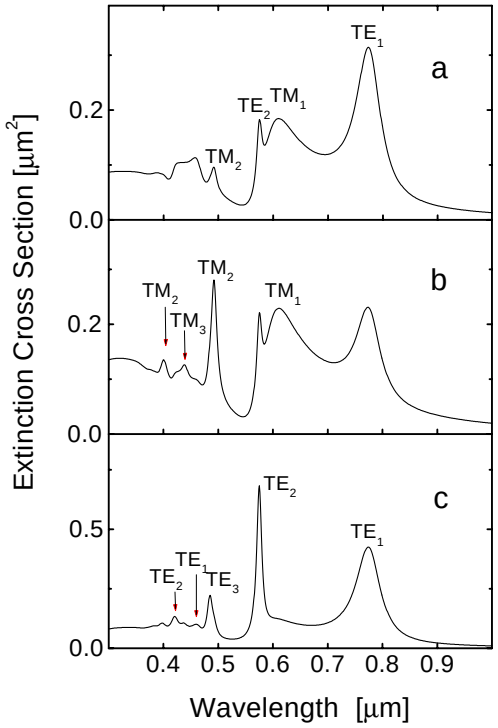

Fig. 1a–c. Spectra of the extinction cross sections for a homogeneous silicon particle in vacuum with $2a = 200$ nm for plane-wave excitation (**a**), and for *p*-polarised (**b**), and *s*-polarised (**c**) evanescent-wave excitation. For the evanescent waves an angle of incidence of 60° of the totally reflected wave and a constant index of refraction of the prism $n_p = 1.5$ is assumed. Note the different scale in Fig. 1c

At this point it is assumed that the particle is in front of the glass prism at a distance d, such that multiple scattering processes involving the prism surface can be neglected. The spectra in Fig. 1 exhibit a number of maxima, which can be assigned to morphology-dependent resonances (MDRs), and the assignment to TM- and TE modes for this sphere is indicated in the figure. As discussed above, the peak positions and half widths of these MDRs are unaffected by the kind of excitation. In contrast to this, the peak heights depend on the excitation. It may be recognized from Fig. 1, that in the case of *p*-polarisation MDRs corresponding to TM_2 multipoles and in the case of *s*-polarisation those corresponding to TE_2 and TE_3 multipoles are strongly enhanced compared to plane-wave excitation. A similar result was reported in [2] for the resonances of a silver sphere with $2a = 200$ nm. Due to the large real part of the refractive index of silicon, however, resonances due to magnetic multipoles cannot be neglected for the silicon sphere of Fig. 1, in contrast to a silver sphere of the same size. This leads to the appearance of TE modes in the spectra, which are strongly excited by the transverse electric *s*-polarised evanescent waves, whereas TM modes are more efficiently excited by the transverse magnetic *p*-polarised waves. The scattering spectra of the silicon particle just considered are qualitatively similar to the extinction spectra. Contributions from multipoles of higher order are, however, relatively weaker than for the extinction cross sections, as the squared absolute values of the Mie coefficients in (1b), (1d) decrease faster with order n than the real parts which appear in (1a), (1c). It should be added, that the optical absorption cross section generally exhibits a stronger contrast between off-resonant and on-resonant conditions than the scattering cross section.

An example of the significant changes that arise in the scattering spectrum of somewhat larger particles due to evanescent-wave excitation is shown in Fig. 2, which displays the scattering cross sections of a spherical diamond particle of diameter $2a = 600$ nm. In this case extinction and scattering cross sections are, of course, identical, as the absorption of pure crystalline diamond vanishes in this range of wavelengths. Sharp MDRs of order $n \leq 7$ in the visible spectrum exhibit again strong enhancements in the evanescent field, and as in the case just discussed, TM modes are favored for *p*-polarised excitation and TE modes for *s*-polarised excitation, the difference increasing with order n of the multipoles. Due to the oscillatory nature of the Riccati–Bessel functions in the denominator of the Mie coefficients, a second set of resonances associated with the same multipolar orders $n \leq 7$ appears at wavelengths shorter than about 400 nm, i.e. at larger size parameters (not shown here). Their enhancements in the evanescent field are similar.

The spectral dependence of the scattering cross sections in Fig. 2 demonstrates clearly the large enhancements of contributions from higher multipoles due to the large field gradients of evanescent waves. Comparing the very large absolute values of the cross sections for evanescent-wave excitation (Fig. 2b,c) to those for plane-wave excitation (Fig. 2a) it should be kept in mind, that the cross sections of (1) have been normalised to equal power incident on the particle and that for such a large particle the evanescent wave decays over only a fraction of the particle diameter.

It should finally be remarked that the field distributions are very different for plane-wave and evanescent-wave exci-

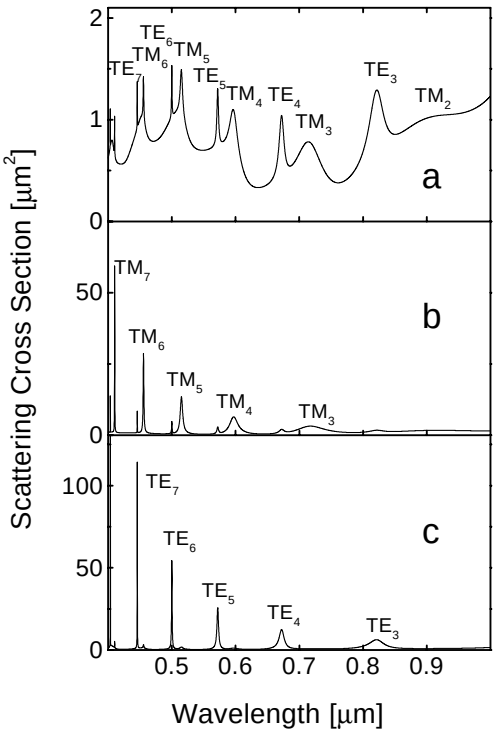

Fig. 2a–c. Scattering spectra of a spherical diamond particle of diameter $2a = 600$ nm for an incident plane-wave (**a**) and for *p*- and *s*-polarised evanescent waves (**b**,**c**), respectively. Evanescent waves as in Fig. 1

tation even when the same resonance is excited. For example, in the case of evanescent-wave excitation the ring-shaped pattern of field nodes corresponding to the MDRs of a homogeneous particle is rotating in the plane of incidence. This is contrary to the case of plane-wave excitation, where two counterpropagating waves are generated which travel close to the inner surface of the sphere and produce a fixed pattern of field nodes. MDRs of high order, so-called whispering gallery modes, have been generated experimentally by evanescent-wave excitation by Collot et al. in view of quantum-optical applications [17].

2.2 Results and discussion for silver-coated spheres

Whereas for homogeneous spheres either large particles or particles with sufficiently large refractive index are required to obtain morphology-dependent resonances, comparatively small particles can exhibit resonances in the visible spectral region, if they are coated by a metal. The position of resonances due to the excitation of collective eigenmodes of the conduction electrons in the metal shell is determined by (12). However, as the absorption in the metal, which is proportional to the imaginary part ε_2, broadens such resonances, ε_2 should be sufficiently small in the spectral range under consideration, if narrow resonances and large cross sections are desired. The smallest values of ε_2 in the visible are found for alkali metals, for example sodium, and for silver. For all other metals ε_2 is significantly larger. Because of its high reactivity with water, sodium cannot be used as coating material under ambient conditions. Thus for practical use silver is most suitable as coating material.

For example, for a silver particle with $2a = 22$ nm ($d = 0$ nm) and a silver-coated silica particle ($2a = 20$ nm, $d = 1$ nm) the resonance conditions for the first three TM modes with multipolar order $n = 1, 2,$ and 3 are calculated using (12) and (13). As the imaginary part of $\varepsilon_{\mathrm{Ag}}$ is rather small in the visible spectral region and does not vary rapidly with the wavelength, it is a good approximation to solve (12) and (13) only for the real part of $\varepsilon_{\mathrm{Ag}}$. For the coated sphere, (12) yields two solutions. This is similar to the case of a thin plane metallic film for which two surface plasmons of different frequency exist due to the interaction of the surface plasmons on each surface [18]. For large shell thickness the long-wave resonance approaches the position of the corresponding resonance for a homogeneous silver particle, i.e. it is related to the interface between the shell and the surrounding medium. Vice versa, the short-wave resonance is related to the inner interface. The values obtained for the sphere are plotted in Fig. 3, where the bulk dielectric constant of silver [19] is plotted versus the vacuum wavelength. It is easily recognized that the resonance positions of the multipoles are clearly separated for the silver-coated particle (squares) whereas the peak positions of the compact silver particle (circles) are close together. The resonance positions for the second solution of (12) are also close to each other and, moreover, are very close to the wavelength where $\varepsilon_{\mathrm{Ag}} = 0$, which is the condition for the bulk plasmon. The discussion so far makes it clear that resonance positions of a silver-coated sphere may be tuned within a wide range of wavelengths by adjusting the core size and the thickness of the shell.

Figure 4 displays the dependence of the extinction spectra of silica particles coated with a silver shell of thickness $d = 10$ nm for the case of p-polarised evanescent-wave excitation and core radii $a = 20$ to 150 nm in 10-nm steps. For clarity the spectra are shifted vertically by a constant amount. The individual multipolar contributions are identified. The line marked with a star arises from all multipoles appearing in the spectrum and corresponds to the resonances close to $\varepsilon_1(\mathrm{Ag}) = 0$, compare Fig. 3. For the smallest core radius of $a = 20$ nm only the dipole contribution is observed. With increasing core size higher multipoles appear and the splitting between the resonance positions increases. At the same time resonances due to lower multipole orders broaden and shift to the red. The resonance at $\lambda \approx 340$ nm corresponding to $\varepsilon_1(\mathrm{Ag}) \approx 0$ remains at approximately the same position for all core sizes. Figure 5 shows the dependence of the observable resonance positions on core size for thickness $d = 1, 2, 5, 10$ nm. The lines through the calculated positions are only guidelines to the eye, but to a good approximation a linear relationship is observed. The compari-

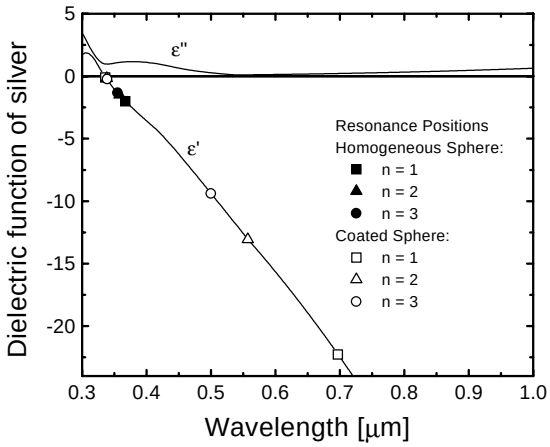

Fig. 3. Resonance positions of Mie coefficients a_n, b_n with $n \leq 3$ for silver spheres of diameter $2a = 22$ nm and for silver-coated silica spheres with core diameter $2a = 20$ nm and shell thickness $d = 1$ nm. The surrounding medium is assumed to be vacuum

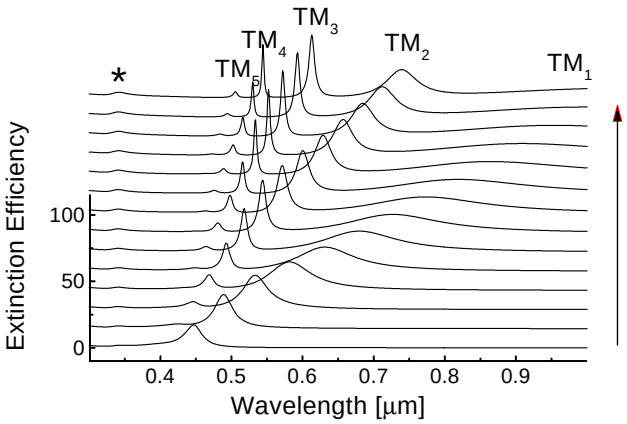

Fig. 4. Extinction spectra of silica particles coated with a silver shell of thickness $d = 10$ nm for p-polarised evanescent-wave excitation and core radius $a = 20$ to 150 nm in 10-nm steps (arrow marks increasing core size). To account for the variation in the cross sections for the different particle sizes the cross sections have been normalised to the particle cross sections to obtain the extinction efficiency. p-polarised wave as in Fig. 2. The *line* marked with a star arises from all multipoles appearing in the spectrum (compare Fig. 3). Again $\varepsilon_{\mathrm{M}} = 1$

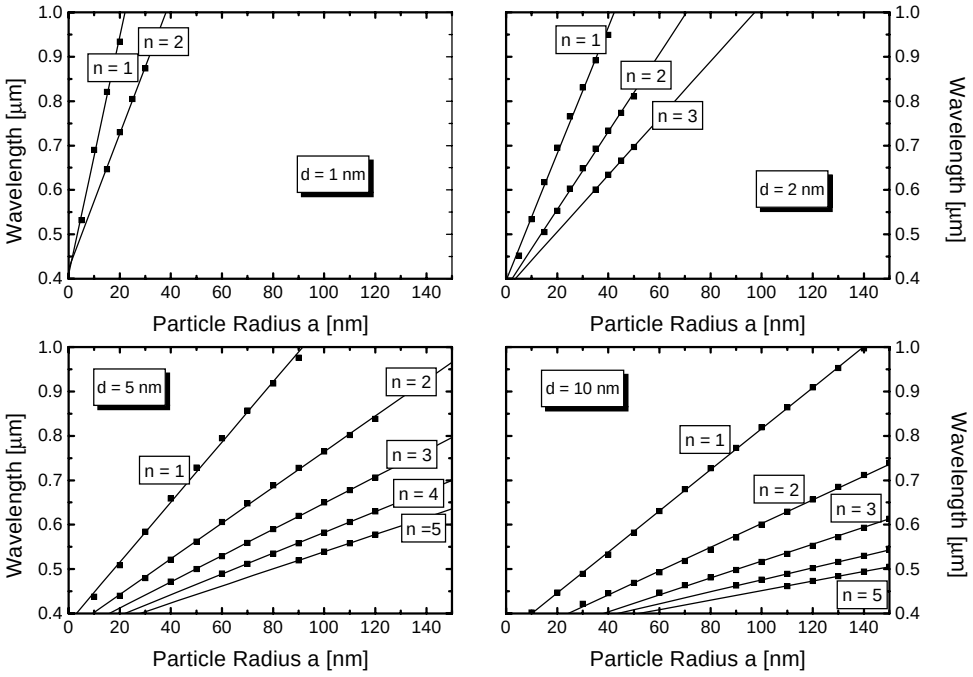

Fig. 5. Resonance positions of the electric multipoles TM_n for silver-coated silica particles as a function of core radius and thickness of the shell. The *straight lines* are guidelines to the eye

son of the resonance amplitudes for the coated particles for plane-wave and evanescent wave-excitation is deferred to the next paragraph.

3 Effects of the prism surface on scattering and extinction spectra

In order to observe scattering or extinction of evanescent waves by small particles, total internal reflection from a prism surface will generally be employed. In this case the interaction of the particle with the prism surface has to be taken into account. This interaction will now be discussed for the representative cases studied in Sects. 2.1 and 2.2. There have been a number of attempts to describe this interaction analytically for the case of plane-wave excitation (compare, for example [20–23] and references therein). A useful approach is to consider the particle to be interacting with its mirror image. In the current paper, however, instead of an analytical treatment, preference was given to the numerical 'multiple multipole (MMP)' method [24] for the study of such multiple scattering processes. This method has been used to calculate the field distributions in the vicinity of the sphere, and from these fields the scattering and extinction cross sections have been calculated as described in [2].

3.1 Homogeneous spheres

The case of the large spherical diamond particle of diameter 2a = 600 nm, already investigated in Sect. 2.1, is best suited to understand the general effects of the prism surface on MDRs of homogeneous particles. Figure 6 shows the scattering spectra of such a particle when it is in contact with the prism surface, either excited by a plane wave incident normally from the prism side or by evanescent waves of either *p*- or *s*-polarisation.

Comparing Fig. 2 and Fig. 6 it may be recognized, that all MDRs are strongly broadened by multiple scattering at the prism surface. This is accompanied by a strong reduction of the peak cross sections. Besides, there is a redshift of the maxima in the range of a few nanometers, decreasing towards higher multipole orders. The broadening of the resonances may be understood as a reduction of the quality factor of the resonances due to the leakage of energy of the resonant mode into the prism. In the presence of the particle total internal reflection is, of course, disturbed, and, correspondingly, the excitation does not contain the large intensity gradient of the undisturbed evanescent wave. This leads to the reduction of the amplitudes of higher-order resonances. The redshift may be explained qualitatively by observing that the near field of the particle extends partly into the prism material with its higher refractive index, and that the Mie resonances shift to longer wavelengths, when a particle is embedded in a medium of higher refractive index. The redshift is larger for TM modes than for TE modes. This may be explained in a heuristic fashion by the fact that for TE modes the electric field is parallel to the surface, which corresponds to a serial arrangement of the impedances of both halfspaces, whereas for TM modes there is a field component normal to the surface, which means that the impedances are parallel. Simplifying the surface as an equivalent electric circuit consisting of two serial or parallel capacitances, respectively, a larger effective dielectric constant for the TM modes is obtained. Comparison of Fig. 2 and Fig. 6 makes it clear that large resonance enhancements are possible, when the particle is held at some distance from the prism surface. On the other hand, even when the sphere is in contact with the surface (Fig. 6) the spectra for evanescent-wave excitation differ strongly from those for plane-wave excitation, and resonances with large peak amplitudes are observed for *s*- as well as *p*-polarised evanescent waves.

While the angular dependence of the scattered intensity is not the main subject of the current paper, Fig. 7 serves

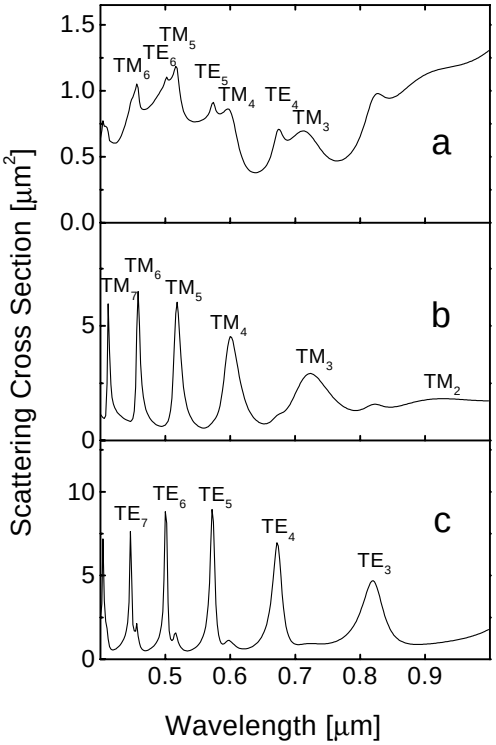

Fig. 6. Scattering spectra for a spherical diamond particle of diameter $2a = 600$ nm in contact with the prism surface. Multiple scattering is included in the calculation. Refractive index of the prism $n_p = 1.5$. Evanescent waves as in Fig. 2. In the plane-wave case a plane wave is assumed to be incident normally on the prism surface from the prism side, and the corresponding transmitted wave excites the particle

to demonstrate the strong changes in the differential cross sections effected by the prism surface. It shows the time-averaged Poynting vector of the *scattered* field for the same diamond particle and for *p*-polarised evanescent-wave excitation with the real part of the wavevector pointing vertically from the top of the figure to the bottom and the evanescent wave decaying from the right to the left. While a nearly isotropic emission is obtained, when multiple scattering at the prism surface is neglected (Fig. 7a), a very directional scattering pattern is obtained when the particle is in contact with the surface (Fig. 7b). The latter is indicated by the vertical line in Fig. 7b, and the prism is to the right of this line. Most of the intensity is scattered in a certain direction into the prism. In the limit of geometrical optics this corresponds to the refraction of the wave propagating close to the inner surface of the sphere into the prism. The emission angle therefore depends on the radius of the sphere and on the order of the MDR.

3.2 Silver-coated spheres

Figure 8 compares the extinction spectra of a silver-coated silica particle of core diameter $2a = 200$ nm and shell thickness $d = 10$ nm when the particle is in contact with the prism surface (straight lines), and when it is far away from the surface, such that multiple scattering processes maybe neglected. Similar to the MDRs considered in the previous section, resonances of higher order are strongly damped in the presence of the surface, but the spectra still differ markedly for

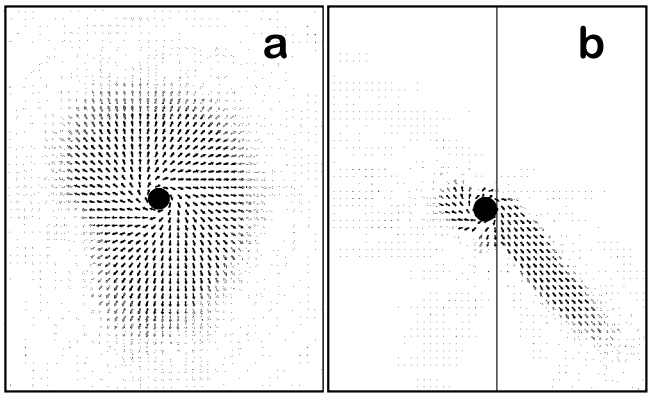

Fig. 7a,b. Time-averaged Poynting vector of the *scattered* field for a diamond particle of radius $a = 300$ nm and for *p*-polarised evanescent-wave excitation at the TM_6 resonance at 456 nm in free space (**a**) , and at 458 nm, when the particle is in contact with the prism surface (**b**). The latter is indicated by the straight line, and the prism is to the right of this line. The evanescent wave propagates from the top of the figure to the bottom and decays from the right to the left

evanescent and plane-wave excitation, and significant resonance enhancements remain for evanescent-wave excitation. It was further found in the MMP calculations, that the multiple-scattering processes become quickly ineffective, when the particle is not in contact with the prism surface, but is held at a short distance to the surface. For instance, for a homogeneous silver particle of radius $a = 100$ nm the scattering and extinction spectra are indistinguishable from those without multiple scattering when the distance exceeds about half the particle radius.

4 Conclusion

Resonance enhancements due to evanescent-wave excitation have been studied for homogeneous and for silver-coated particles. In the case of the so-called morphology-dependent resonances very strong polarisation-dependent enhancements

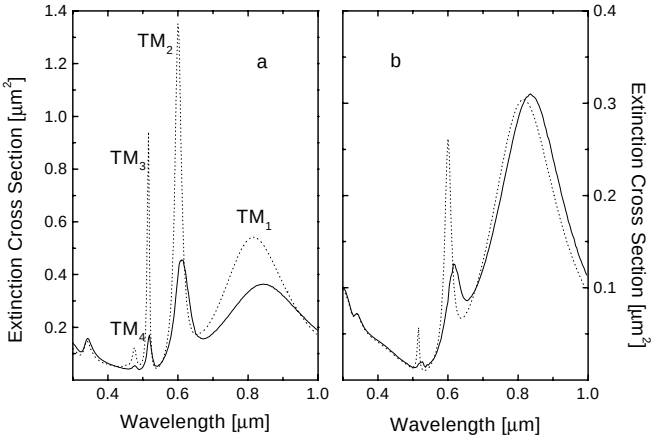

Fig. 8a,b. Extinction spectra of a spherical silver-coated silica particle in contact with the prism surface (*straight lines*) and far away from the surface (*dotted lines*). Core diameter $2a = 200$ nm, shell thickness $d = 10$ nm, $n_p = 1.5$. **a** Evanescent-wave excitation, parameters as in Fig. 2. **b** Excitation by a plane wave incident normally from the prism side

are found. For silver-coated particles the resonances may be tuned throughout the visible spectrum by varying the core size and refractive index of the particle. Multiple-scattering processes at the prism surface reduce the resonant cross sections significantly. In addition, a broadening and a redshift occur, when the particle is in contact with the prism surface. Furthermore, the angular distribution of the scattered light becomes highly anisotropic in this case. Even then, however, the scattering and extinction spectra differ strongly for evanescent and plane-wave excitation and the stronger resonances in the former case may be useful for a number of practical applications.

Acknowledgements. Financial support from the Deutsche Forschungsgemeinschaft (Innovationskolleg 'Methods and Materials for the Nanometer Range') is gratefully acknowledged.

References

1. G. Mie: Ann. Phys. **25**, 377 (1908)
2. M. Quinten, A. Pack, R. Wannemacher: Appl. Phys. B, in print 1998
3. H.C. van de Hulst: *Light Scattering by Small Particles* (Wiley, New York 1957)
4. M. Kerker: *The Scattering of Light and Other Electromagnetic Radiation* (Academic Press, New York 1969)
5. C.F. Bohren, D.R. Huffman: *Absorption and Scattering of Light by Small Particles* (Wiley, New York 1983)
6. J.A. Stratton: *Electrodynamic Theory* (McGraw Hill, New York 1941)
7. P. Debye: Ann. Phys. **30**, 57 (1909)
8. H. Chew, D.S. Wang, M. Kerker: Appl. Opt. **18**, 2679 (1979)
9. C. Liu, T. Kaiser, S. Lange, G. Schweiger: Opt. Commun. **117**, 521 (1995)
10. D. Barchiesi, D. van Labeke: J. Mod. Opt. **40**, 1239 (1993)
11. A.L. Aden, M. Kerker: J. Appl. Phys. **22**, 1242 (1951)
12. A. Güttler: Ann. Phys. **11**, 65 (1952)
13. R. Bhandari: Appl. Opt. **24**, 1960 (1985)
14. J. Sinzig, M. Quinten: Appl. Phys. A **58**, 157 (1994)
15. L. Kai, P. Massoli: Appl. Opt. **33**, 501 (1994)
16. E.D. Palik (Ed.): *Handbook of Optical Constants of Solids* (Academic Press, New York 1996)
17. L. Collot, V. Lefèvre-Seguin, M. Brune, J.M. Raimond, S. Haroche: Europhys. Lett. **23**, 327 (1993)
18. H. Raether: *Excitation of Plasmons and Interband Transitions by Electrons*, Springer Tracts in Modern Physics 88 (Springer, Berlin, Heidelberg 1980)
19. M. Quinten: Z. Phys. B **101**, 211 (1996)
20. P.A. Bobbert, J. Vlieger: Physica A **137**, 209 (1986)
21. G. Videen, M.G. Turner, V.J. Iafelice, W.S. Bickel, W.L. Wolfe: J. Opt. Soc. Am. A **10**, 118 (1993)
22. B.R. Johnson: J. Opt. Soc. Am. A **13**, 326 (1996)
23. E. Fucile, P. Denti, F. Borghese, R. Saija, O.I. Sindoni: J. Opt. Soc. Am. A **14**, 1505 (1997)
24. Ch. Hafner: *The Generalized Multipole Technique for Computational Electromagnetics* (Artech House Books 1990)